Terrestrial Data for Calibration and Error Assessment of GOCE Gravity Gradients

J. Bouman, R. Koop

SRON National Institute for Space Research, Utrecht, The Netherlands
N. Sneeuw

Department of Geomatics Engineering, University of Calgary, Calgary, Canada
C.C. Tscherning

Department of Geophysics, University of Copenhagen, Copenhagen, Denmark

Camera-ready Copy for

Presented at EGS/EUG/AGU meeting 2003

Manuscript-No. ???

Presented at EGS/EUG/AGU meeting 2003 (2003) #:1–7

Terrestrial Data for Calibration and Error Assessment of GOCE Gravity Gradients

J. Bouman, R. Koop

SRON National Institute for Space Research, Utrecht, The Netherlands

N. Sneeuw

Department of Geomatics Engineering, University of Calgary, Calgary, Canada

C.C. Tscherning

Department of Geophysics, University of Copenhagen, Copenhagen, Denmark

Received: ??? – Accepted: ???

Abstract. GOCE will be the first satellite mission ever measuring gravity gradients using a dedicated instrument called a gradiometer. High resolution gravity field recovery will be possible from these gradients under the condition that systematic errors have been removed to the extent possible from the data and the gravity gradients accuracy has been assessed. Regional terrestrial gravity data with high resolution and high accuracy could possibly be used for these purposes. As an example, we will show how Canadian gravity data can be used for the external calibration of the gravity gradients, that is, correcting the gradients for systematic effects, and how the gravity gradient error can be assessed with these terrestrial data. In this study we estimated one bias for each satellite ground track in the region with terrestrial data using least-squares collocation (LSC) with parameters. The estimated bias as well as the calibrated gravity gradients have high accuracy. In addition, it is shown that the LSC predicted gravity gradients from the terrestrial data have an accuracy level comparable to that of the observed GOCE gravity gradients. Hence error assessment is possible.

1 Introduction

The main goal of the GOCE mission (expected to be launched early 2006) is to provide unique models of the Earth's gravity field and of its equipotential surface, as represented by the geoid, on a global scale with high spatial resolution and to very high accuracy (ESA, 1999). To this end, GOCE will be equipped with a GPS receiver for high-low satellite-to-satellite tracking (SST-hl) observations, and with a gradiometer for observation of the gravity gradients (SGG). The gradiometer consists of six 3-axes accelerometers mounted in pairs along three orthogonal arms. From the readings of each pair of accelerometers the so-called common mode (CM) and differential mode (DM) signals are derived. The CM observations are used to obtain information about the linear accelerations and are input to the drag free control system. The measurements of the CM are also needed for accurate separation of the non-conservative and conservative forces and are therefore important for the long wavelength gravity field recovery from SST measurements. The DM observations are used to derive the gravity gradients. The accelerometers and the gradiometer are designed such as to give the highest achievable precision in the measurement bandwidth (MBW) between 5 and 100 mHz. For the diagonal gravity gradients in a Local Orbital Reference Frame (LORF, x-axis in the velocity direction, the z-axis approximately radially outward and the y-axis complements the right-handed frame) this precision will not exceed 4 mE/$\sqrt{\text{Hz}}$ (1 E = 10^{-9} s^{-2}) in the MBW (Cesare, 2002).

The observations will be contaminated with stochastic and systematic errors. For the GOCE gradiometer, systematic errors typically are due to instrument imperfections like misalignments of the accelerometers, scale factor mismatches etc. The CM and DM couplings, which are the result of such instrument imperfections, can be determined to an accuracy level of $10^{-2} - 10^{-4}$ prior to the mission by the so-called pre-flight calibration on ground using a test bench (Cesare, 2002). In orbit, a so-called internal (in-flight) calibration procedure will be used (ESA, 1999), by which the CM and DM couplings can be determined to an accuracy level at which their effect on the gradients in the MBW stays below the required 4 mE/$\sqrt{\text{Hz}}$. The values of the calibration parameters (elements of the calibration matrix) are measured by putting a known acceleration signal on the gradiometer in orbit using the thrusters. After this procedure, the CM and DM read-outs of the gradiometer are corrected using the measured calibration parameters.

The gravity gradients are derived from the internally calibrated DM accelerations. The internal calibration, however, is not sensitive to all instrument imperfections. The read-out bias, for example, and the accelerometer mis-positioning cannot be accounted for. Therefore, in order to possibly correct for remaining errors after internal calibration, a third calibration step is required which is called external calibration (or absolute calibration). It is performed during or after the mission and typically makes use of external gravity data, e.g.

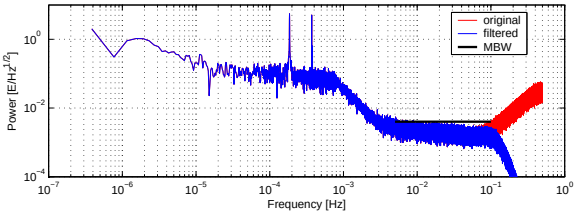

Fig. 1. SD of V_{zz} gravity gradient errors after internal calibration and filtering.

terrestrial gravity data or global gravity field models (Arabelos and Tscherning, 1998; Koop et al., 2002).

Along with the external calibration of the observations, their error needs to be assessed. For this purpose we could again use terrestrial gravity data. Alternatively, we could use the GOCE data themselves and perform an internal assessment, but this is not discussed here, see e.g. (Albertella et al., 2000; Koop et al., 2002; Bouman and Koop, 2003).

Before we can reliably use terrestrial data in the calibration and error assessment of GOCE gravity gradients, we need to assess these data themselves. It is well known, e.g., that (unknown) long wavelength errors can occur in these data, e.g. due to regional datum offsets. Moreover, the gravity anomalies as well as their error model need to be upward continued and converted to gravity gradients if we want to use them for external calibration and error assessment. Also the regional area with high quality terrestrial data needs to be large enough to assess the gradient error in the MBW. As a rule of thumb, the minimum size of region must correspond to 200 s or 1600 km approximately.

The simulation of the GOCE gravity gradients is discussed in Section 2, while the generation of the terrestrial gravity data is discussed in Section 3. In Section 4 the calibration is detailed and Section 5 deals with error assessment.

2 Simulated gradiometric data

A GOCE-like orbit was generated with an inclination of $96.6°$ and a semi-major axis of approximately 6648 km or 270 km above the Earth's surface. The orbit had a repeat period of 2 months of which for the first month gravity gradients along the orbit were computed with a sampling of 1 s. EGM96 (Lemoine et al., 1998) complete up to degree and order $L = 360$ was used to generate 'true' gravity gradients. The gravity gradients as observed by GOCE after internal calibration were simulated with SRON's E2E instrument simulator, which includes mis-alignments, cross-couplings etc. (SID, 2000). The high frequency errors were filtered using a third-order lowpass Butterworth filter with a cut-off frequency of 0.11 Hz, which is just above the MBW. The 'measured' gravity gradients were filtered in both the forward and the reverse directions to remove all phase distortion, effectively doubling the filter order. As an example the spectral density (SD) of the V_{zz} errors is shown in Figure 1.

A region was selected where terrestrial gravity data are

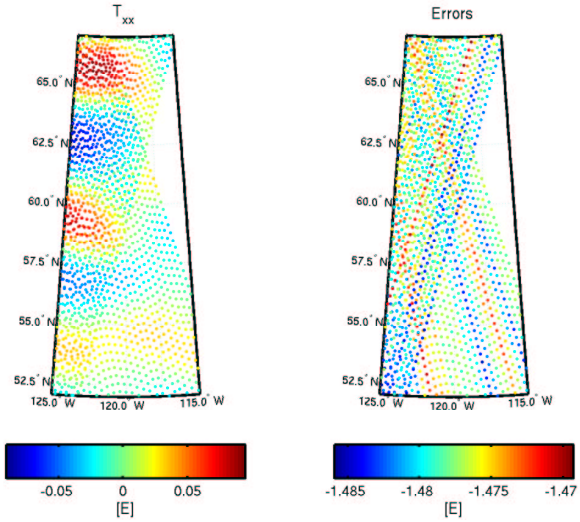

Fig. 2. True T_{xx} signal in the LORF, EGM96, $l = 51 - 360$ (left panel). Filtered E2E errors (right panel).

available to calibrate the gravity gradients, see below. The gravity gradients on the 55 tracks over this region were downsampled from 1 s to 5 s (every 5th observation was used). Due to the filtering all signal and noise above 0.1 Hz has been removed, which justifies the downsampling. Since the long wavelength gravity field can not be represented well by regional data, EGM96 up to degree and order $L = 50$ was subtracted from the true and observed gradients. Shown in Figure 2 are the true reduced T_{xx} gravity gradients in the LORF as well as the errors. The errors have a large mean but a small standard deviation, see Table 1. The offset is more or less constant per track, and it is the sum of an instrumental scale factor error, a bias and the errors at 1 and 2 cpr (see the two peaks in Figure 1). The latter appear to be constant in a small region and they result in large error correlation lengths. We computed the empirical error covariance functions of the errors, and these show that the correlation length (where the error covariance is half the variance) is approximately 560 s.

3 Terrestrial gravity data

3.1 Selection criteria for the calibration region

Ideally, a terrestrial data set should contain gravity measurements with high spatial resolution and high accuracy. Such data are not available globally, but they are available for, e.g. Europe or North America. The larger the region with terrestrial data, the better the calibration parameters can be de-

Table 1. Mean and standard deviation of the errors in the observed gravity gradients (1528 data points).

gradient	mean [E]	σ [mE]
T_{xx}	-1.478	3.0
T_{yy}	-0.813	3.8
T_{zz}	+2.291	3.6

termined, and the larger is the frequency range for the error assessement. If we would, for example, determine a trend for each track, then this trend can be more accurately determined with a longer time interval. If we want to assess the gravity gradient error in the entire MBW, then the longest wavelength is 200 s (1600 km). So, the *inner* region with gravity data should be at least 15° in north-south direction given the fact that the GOCE tracks are approximately north-south due to the almost polar orbit of GOCE. The east-west extension should be such that a sufficient number of tracks enter the error assessment (e.g. 50 tracks), to ensure that the results have statistical relevance. The *outer* region with gravity data should be large enough to achieve a small and homogeneous error in the inner region. The larger the outer region, the more reliable the upward continuation is, see also (Denker, 2002; Müller et al., 2002).

3.2 Real data and filtering

As a limited region is used, the long wavelengths cannot be accurately described by the regional data. Therefore, global long wavelength information has to be subtracted to reduce possible 'leakage'. EGM96, $L \leq 50$, will be used as reference model. In addition, a statistically more homogeneous signal variance is obtained. In a way, subtracting EGM96 acts as a kind of high-pass filter because low frequencies are removed. This is, however, not exactly true since low frequency (instrument) errors remain.

A problem encountered in simulation studies are the inherent differences between a created true world (EGM96) and real terrestrial data. Such differences might be caused by e.g. long wavelength errors (biases, trends) in EGM96 and in the terrestrial data, height datum errors in the terrestrial data, the use of gravity reductions and corrections, etc. The handling of such topics will be part of subsequent research.

Filters have to be designed and applied focussing on the MBW or not. Especially some long-wavelength features (biases, trends) of the surface data are not favorable for high-resolution analysis and one could try to deal with these by filtering. One idea would be to predict gradients in the GOCE observation points from the ground data and then to filter both predicted and observed gradients with a suitable bandpass filter, but this is not further discussed here.

The differences in spectral and spatial information content between the terrestrial data and the GOCE observations could make a proper comparison (in the context of error assessment) between predicted and observed gradients difficult. Also this problem might be solved by proper bandpass filtering.

3.3 Gravity gradient prediction using LSC

When terrestrial gravity data are available, it is possible to predict from it gravity gradients in the LORF. One of the methods to do so is least-squares collocation (LSC), see (Tscherning, 1976, 1993). We use the GRAVSOFT package in our computations (Tscherning, 1974). In view of the problems discussed in the previous section, we did not use true gravity data but generated test data ourselves instead.

Table 2. Statistics of the errors in the LSC predicted gravity gradients (1528 data points): predicted minus true. Gravity anomalies with 1 mGal error were used in the prediction (8601 data points). Between brackets are the LSC predicted standard deviations. Units are [mE].

gradient	mean	σ	min	max
T_{xx}	+0.1	0.6 (0.6)	-1.6	1.7
T_{yy}	+0.2	0.5 (0.7)	-1.3	1.2
T_{zz}	-0.3	0.9 (1.0)	-2.0	2.4

First of all, 'true' gravity anomalies were computed using EGM96, $L = 51 - 360$. The data points lie on a grid with $-135^\circ \leq \lambda \leq -105^\circ$, $42^\circ \leq \phi \leq 77^\circ$, and $\Delta\lambda = 1/2^\circ, \Delta\phi = 1/4^\circ$ (8601 points in total). Errors were added to these data which were uncorrelated with zero mean and a standard devation of 1 mGal. Secondly, an empirical covariance function of the noisy gravity data was determined and an analytical model was fitted to this empirical function (Knudsen, 1987). The variance of the gravity data is 207 mGal^2, so the signal in this region is rather smooth. Finally, we predicted T_{xx}, T_{yy} and T_{zz} in the LORF.

The statistics of the differences between the LSC predicted gravity gradients and the true gravity gradients are shown in Table 2. The differences (errors) are caused by the 1 mGal error on the terrestrial data in combination with model errors such as spherical approximation in LSC and the use of a limited region in the computations. The errors in the predicted gradients are small with almost zero mean and an error standard deviation of 1 mE. The predicted standard deviations from LSC are given between brackets and they closely resemble the true standard deviations σ (3rd column of Table 2). Given the simulated GOCE gradient errors of 3-4 mE, it is therefore feasible to calibrate these gradients using LSC and our simulated ground data.

4 External calibration

Given the gradiometer instrument characteristics, we would like to determine global calibration parameters, that is, calibration parameters valid for the whole time series of gravity gradients. Koop et al. (2002) determine a bias, a scale factor, a trend and Fourier coefficients for 1 and 2 cpr for each diagonal gravity gradient. However, as discussed above, it is not possible to discriminate between, e.g. a bias and 1 and 2 cpr effects in limited regions. In this study, we therefore estimated one bias per track, and could add a trend for each track and, for example, one scale factor for the whole region.

The calibration parameters may be determined in several ways, e.g. using LSC with parameters (Moritz, 1980), or using a mixed model with condition equations (Bouman and Koop, 2002). We will mainly use LSC with parameters in this study. Consider the linear model

$$E\{\underline{t}\} = Ap + t \tag{1}$$

where t is a linear functional of the anomalous gravitational

potential (underlined means observed with noise or estimated from noisy observations), and A represents the effect of the parameters p on $\underline{t}$. We could for example determine 55 bias parameters $p_i, i = 1, \ldots, 55$. The LSC estimate of the parameters is

$$\underline{\hat{p}} = (A^T \bar{C}^{-1} A)^{-1} A^T \bar{C}^{-1} \underline{t} \tag{2}$$

where $\bar{C} = C_{tt} + C_{nn}$ is the total covariance matrix with C_{tt} the signal covariance matrix and C_{nn} is the error covariance matrix of the observations. In contrast to usual least-squares adjustment, the signal covariance matrix plays its role here. Any other linear functional s of the anomalous potential is estimated with

$$\underline{\hat{s}} = C_{st} \bar{C}^{-1} (\underline{t} - A\underline{\hat{p}}) \tag{3}$$

where C_{st} is the cross covariance between t and s. One condition the signals s and t have to fulfil is that their average is zero. This will not necessarily be true for a limited region, however, the larger the region is, the more likely it is that the average is zero, at least for anomalous quantities.

Note that it is possible to estimate (bias) parameters using only the biased gravity gradients, Eq. (2). The additional information needed is the signal covariance function. In principle, it is possible to determine a local covariance function from the observed gravity gradients, but we will use the covariance function as determined from the terrestrial data.

4.1 Bias per track

Gravity gradient biases were estimated, for all three diagonal components, using (2). Different combinations of observations were used, with an assigned uncertainty of 5 mE for the gravity gradients (cf. Table 1) and 1 mGal for the ground data. The bias errors per track (that is, the differences between the LSC predicted bias and the true bias) for the different cases are shown in Figures 3 – 5, while the statistics of these errors are listed in Tables 3 – 5. The 'true' bias is simply the mean simulated gravity gradient error per track (see also Figure 2), which is a lumped bias (sum of several instrumental errors). For comparison, we have determined the gravity gradient biases per track using the LSC predicted gradients from ground data only, hence not using LSC with parameters, as follows: bias = mean($T_{ii}(GOCE) - T_{ii}(LSC)$). Thus the measurement errors were not taken into account here. See last rows of Tables 3 – 5.

All bias errors are small. The errors decrease for increasing number of points per track, see Figure 6. The predicted error is somewhat pessimistic compared to the true bias errors, see Figure 3 and Tables 3 - 5. If the gravity gradient itself is used in the bias estimation, then the results are somewhat degraded compared to a combination of observations or using only Δg (but the results are still satisfactory). The estimated biases using combinations of observations strongly resemble each other. The added value of Δg becomes especially apparent for tracks with few data points.

The statistics of the errors in the calibrated gradients for the different cases are given in Table 6, and one example is

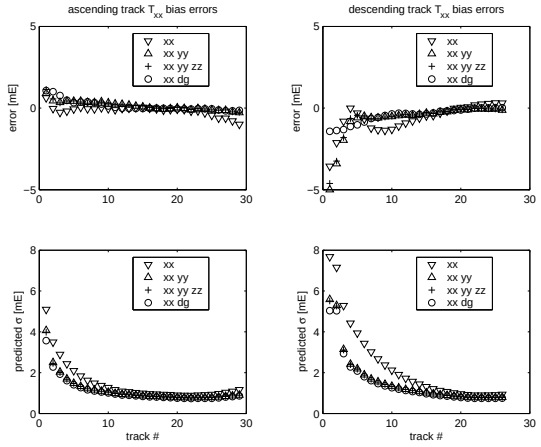

Fig. 3. T_{xx} bias errors (top panels) and predicted error of the biases (bottom panels).

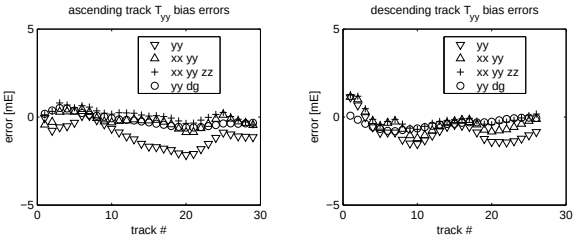

Fig. 4. T_{yy} bias errors.

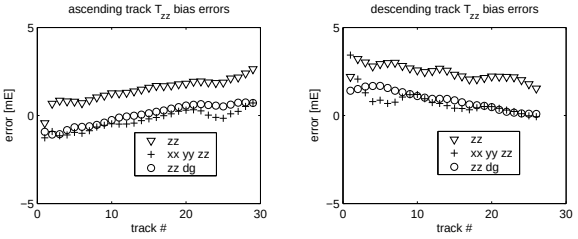

Fig. 5. T_{zz} bias errors.

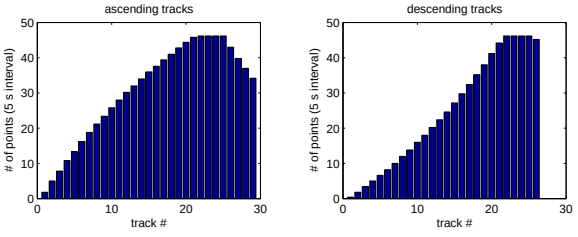

Fig. 6. Number of points per track, ascending tracks (left panel) and descending tracks (right panel). Tracks are numbered from west to east.

Table 3. T_{xx} bias error statistics: predicted minus true. Between brackets are the predicted standard deviations. Units are [mE].

	ascending tracks (29)				descending tracks (26)			
observation	mean	σ	min	max	mean	σ	min	max
T_{xx}	-0.2	0.3 (1.5)	-1.0	0.6	-0.6	0.9 (2.3)	-3.4	0.3
T_{xx}, T_{yy}	+0.1	0.3 (0.7)	-0.3	0.9	-0.7	1.1 (1.3)	-5.0	-0.1
T_{xx}, T_{yy}, T_{zz}	+0.2	0.3 (1.1)	-0.3	1.1	-0.6	1.0 (1.6)	-4.6	0.0
$T_{xx}, \Delta g$	+0.1	0.3 (1.1)	-0.2	1.1	-0.5	0.5 (1.5)	-1.4	0.0
Δg	+0.1	0.4 (-)	-0.2	1.4	-0.4	0.6 (-)	-1.6	0.0

Table 4. T_{yy} bias error statistics: predicted minus true. Between brackets are the predicted standard deviations. Units are [mE].

	ascending tracks (29)				descending tracks (26)			
observation	mean	σ	min	max	mean	σ	min	max
T_{yy}	-1.1	0.7 (2.4)	-2.2	0.1	-0.8	0.6 (2.9)	-1.5	1.1
T_{xx}, T_{yy}	-0.2	0.3 (2.1)	-0.9	0.5	-0.4	0.5 (2.3)	-1.2	1.1
T_{xx}, T_{yy}, T_{zz}	+0.1	0.3 (1.9)	-0.4	0.8	-0.1	0.5 (2.2)	-0.7	1.3
$T_{yy}, \Delta g$	-0.2	0.3 (1.1)	-0.6	0.5	-0.4	0.3 (1.5)	-0.8	0.1
Δg	-0.1	0.3 (-)	-0.6	0.6	-0.2	0.3 (-)	-0.8	0.2

Table 6. Statistics of the errors in the predicted gradients after calibration: predicted minus true. Units are [mE].

	T_{xx}		T_{yy}		T_{zz}	
observation	mean	σ	mean	σ	mean	σ
T_{ii}	-0.2	0.8	-1.2	0.8	1.9	1.0
T_{xx}, T_{yy}	-0.2	0.2	-0.4	0.4	-	-
T_{xx}, T_{yy}, T_{zz}	-0.1	0.2	-0.2	0.4	0.3	0.4
$T_{ii}, \Delta g$	-0.1	0.5	-0.3	0.1	0.6	0.2

shown in Figure 7. The mean error of the calibrated gradients is almost zero for all cases, while the error standard deviation is at the mE-level. Note that the error σ's have become smaller compared to the error in the observed gradients, also when only the gradients were used in the calibration. This is due to the fact the LSC takes the signal correlation into account and smooths the data.

4.2 Bias and trend per track

Besides estimating one bias per track, we could also estimate one bias and a trend per track, see Table 7. Bias and trend could not be estimated for the first two descending tracks (too few data points). When only T_{zz} gradients are used as observations, the results are bad, probably caused by an unstable system of equations. The reason might be that the track length is too short to estimate a trend. When ground data are added, there is improvement, but the errors are still too large.

Table 7. T_{zz} bias error statistics estimating bias and trend: predicted minus true. Units are [mE].

	ascending (29)		descending (24)	
observation	mean	σ	mean	σ
T_{zz}	2.5	1282	-1686	726.3
$T_{zz}, \Delta g$	9.3	13.9	-46.2	35.3

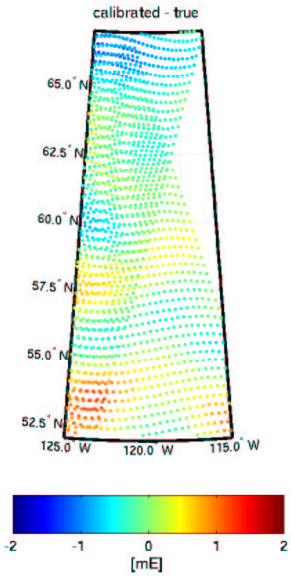

Fig. 7. Errors in the calibrated T_{xx} gradients. Observations were Δg and the original T_{xx} gradients.

Table 8. T_{xx}, T_{yy} and T_{zz} bias error statistics taking gravity gradient error correlation into account: predicted minus true. Units are [mE].

		ascending (29)		descending (26)	
observation	pred.	mean	σ	mean	σ
T_{xx}, T_{yy}, T_{zz}	T_{xx}	9.9	62.2	0.4	57.2
	T_{yy}	27.6	5.3	31.8	6.5
	T_{zz}	-35.1	3.9	-32.8	6.5
$T_{xx}, T_{yy}, T_{zz}, \Delta g$	T_{xx}	0.1	0.3	-0.5	0.4
	T_{yy}	-0.1	0.3	-0.4	0.3
	T_{zz}	0.0	0.6	0.9	0.5
$T_{zz}, \Delta g$	T_{zz}	0.0	0.6	0.9	0.5

Table 5. T_{zz} bias error statistics: predicted minus true. Between brackets are the predicted standard deviations. Units are [mE].

	ascending tracks (29)				descending tracks (26)			
observation	mean	σ	min	max	mean	σ	min	max
T_{zz}	+1.5	0.6 (2.5)	-0.4	2.6	+2.4	0.4 (2.7)	1.5	3.2
T_{xx}, T_{yy}, T_{zz}	-0.3	0.5 (1.9)	-1.3	0.7	+0.8	0.7 (2.2)	-0.1	3.4
$T_{zz}, \Delta g$	+0.0	0.6 (1.2)	-1.1	0.7	+0.9	0.5 (1.5)	0.1	1.7
Δg	+0.0	0.7 (-)	-1.7	0.7	+0.6	0.7 (-)	-0.2	1.8

4.3 Correlated gravity gradient errors

So far the gravity gradient error correlation was not taken into account. However, the errors are correlated and it is possible to account for the correlation, see also (Arabelos and Tscherning, 1999). Since the error correlation length is long, 560 s, compared to the maximum track length, < 250 s, all errors on one track will be heavily correlated. Consequently, the associated error matrix C_{nn} will be full and it might be (numerically) singular. Therefore, when only gravity gradients are used as observations, bias estimates or any other estimate may be unreliable. The addition of ground data may improve the solution. Results are shown in Table 8, and indeed using only gradients does not lead to accurate bias estimates. Although the bias errors do not exceed several tens of mE, we consider them too large. Using also ground data dramatically improves the bias recovery. The combination $T_{zz}, \Delta g$ is (almost) identical to results without error correlation.

5 Error assessment

In general observational errors may be assessed by comparing the obserations with predicted observations. The predicted observations could be based on terrestrial gravity data converted to the correct quantity, which is called external error assessment. We will discuss the generic error assessment model and detail its specific form for external error assessment.

5.1 Generic model

The model of condition equations is

$$B^T E\{\underline{y}\} = 0; \;\; D\{\underline{y}\} = Q_y \tag{4}$$

with least squares errors

$$\underline{\hat{e}} = Q_y B (B^T Q_y B)^{-1} B^T \underline{y}. \tag{5}$$

The gravity gradients $\underline{y}$ are the calibrated GOCE observations, as well as those derived from independent data. The error variance-covariance matrix Q_y is full in general, for example due to the coloured noise behaviour of the gradiometer the gravity gradient errors will be correlated in time.

An unbiased estimate of the variance of unit weight is

$$\underline{\hat{\sigma}}^2 = \frac{\underline{\hat{e}}^T Q_y^{-1} \underline{\hat{e}}}{b} \tag{6}$$

with b the rank of B, that is, the number of independent condition equations. Thus $\underline{\hat{\sigma}}^2$ depends on the a priori error matrix Q_y and the a posteriori error $\underline{\hat{e}}$. In practice one could use (6) to test whether one a priori error model is to be preferred over the other. The closer $\underline{\hat{\sigma}}^2$ is to 1, the more likely it is that the corresponding a priori model Q_y describes the errors well. Note that it is assumed that outliers have been removed.

The distribution of $\underline{\hat{\sigma}}^2$ under the null hypothesis H_0 (i.e. the a priori error model is correct) is given as

$$H_0 : \underline{\hat{\sigma}}^2 \sim F(b-1, \infty) \tag{7}$$

that is a central F distribution. The a priori error model will be rejected if

$$\underline{\hat{\sigma}}^2 > k_{\alpha/2}$$

(a priori error model is too optimistic) or

$$\underline{\hat{\sigma}}^2 < k_{1-\alpha/2}$$

(a priori error model is too pessimistic), that is, if the a posteriori variance of unit weight is larger or smaller than a critical value with significance level $\alpha/2$. E.g. $F_{0.025}(59, \infty) = 1.49$ and $F_{0.975}(59, \infty) = 0.72$, which means that for 60 conditions equations the a priori error model will be rejected if the a posteriori variance of unit weight is larger than 1.49 or smaller than 0.72. In approximately 5 % of the cases the null hypothesis will be rejected although the a priori error models are correct.

5.2 Error assessment with terrestrial data

The idea behind error assessment with terrestrial data is quite straightforward: take the difference between observed gradients and gradients derived from terrestrial data. Ideally, this difference is only due to observational errors and if the a priori error models of both observation types are correct then these differences should be predicted reasonably well by the error models. If not, then one or both of the error models are incorrect. Let's group the observed and predicted gradients in one vector y_k, $k = 1, \ldots, 2m$ where the first m elements are the calibrated gradients and the second m observations are the predicted gradients. The condition equations then take the form

$$E\{y_i - y_{i+m}\} = 0, \;\; i = 1, \ldots m. \tag{8}$$

The error matrix Q_y contains the two error matrices corresponding to the calibrated and predicted gradients.

It is important to note that the accuracy of the predicted gravity gradients needs to be at the same level as the observed

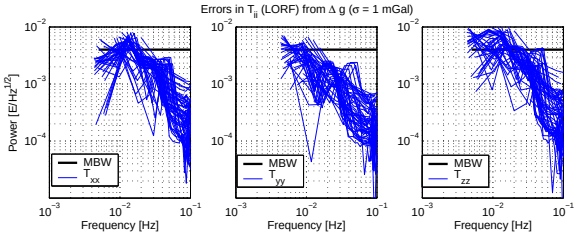

Fig. 8. SD of the errors in the LSC predicted gravity gradients.

gravity gradients. For example, if the gradient errors are uncorrelated and the observed gradients have equal variance σ_1^2 and the predicted gradients have equal variance σ_2^2, then the variance of unit weight (6) becomes

$$\hat{\underline{\sigma}}^2 = \frac{1}{m}\frac{1}{\sigma_1^2+\sigma_2^2}\sum_{i=1}^{m}(y_i - y_{i+m})^2. \qquad (9)$$

Would σ_2^2 be much larger than σ_1^2 then our test is not sensitive to changes in σ_1^2, which is the a priori error model we wish to examine.

5.3 Results

In Figure 8 the SD of the differences between true and predicted gravity gradients are shown. The LSC predicted gradients used Δg as observations (see also Table 2). The SD of the errors for each track are shown and the error of the predicted gradients is at the level of the MBW, which is what is needed for error assessment. Hence it is possible to use the predicted gradients in the error assessment of the (calibrated) observed gradients.

6 Conclusions and discussion

Bias parameters can be accurately determined using LSC and ground data, down to the mE-level. It is even possible to determine bias parameters using only the observed gravity gradients. The underlying assumptions are that the true anomalous gravity gradients in a region are centered (mean = 0) and that we can derive a local covariance function from the observed gradients. The error of the calibrated gradients is small (mE).

Due to the extreme correlation length, the system of equations becomes unstable if the error correlation is accounted for and if only the gravity gradients themselves are used as observations. Adding ground data stabilizes the solution and bias parameters can be estimated. Estimating bias and trend is difficult due to the short track length. Ground data improves the solution, but not enough.

The accuracy of the observed gravity gradients and the predicted ones using ground data is at the same level. It is therefore possible to assess the error of the observed gravity gradients if the error of the predicted gradients is predicted accurately.

Acknowledgements. José van den IJssel (DEOS, DUT) computed the GOCE orbit, which is acknowledged. Volker Hannen (SRON) simulated the gravity gradient errors, which is acknowledged as well.

References

Albertella, A., Migliaccio, F., Sansò, F., and Tscherning, C., Scientific data production quality assessment using local space-wise pre-processing, in *From Eötvös to mGal, Final Report*, edited by H. Sünkel, ESA/ESTEC contract no. 13392/98/NL/GD, 2000.

Arabelos, D. and Tscherning, C., Calibration of satellite gradiometer data aided by ground gravity data, *Journal of Geodesy*, *72*, 617–625, 1998.

Arabelos, D. and Tscherning, C., Gravity field recovery from airborne gradiometer data using collocation and taking into account correlated errors, *Physics and Chemistry of the Earth, 24*, 19–25, 1999.

Bouman, J. and Koop, R., Calibration of GOCE SGG data combining terrestrial gravity data and global gravity field models, Accepted for publication in *Proceedings of the 3rd meeting of the IGGC*, Thessaloniki, Greece, 2002.

Bouman, J. and Koop, R., Error assessment of GOCE SGG data using along track interpolation, Accepted for publication in *Advances in Geosciences*, 2003.

Cesare, S., Performance requirements and budgets for the gradiometric mission, Issue 2 GO-TN-AI-0027, Preliminary Design Review, Alenia, 2002.

Denker, H., Computation of gravity gradients for Europe for calibration/validation of GOCE data, Accepted for publication in *Proceedings of the 3rd meeting of the IGGC*, 2002.

ESA, Gravity Field and Steady-State Ocean Circulation Mission, Reports for mission selection; the four candidate earth explorer core missions, ESA SP-1233(1), 1999.

Knudsen, P., Estimation and modelling of the local empirical covariance function using gravity and satellite altimeter data, *Bulletin Géodésique*, *61*, 145–160, 1987.

Koop, R., Bouman, J., Schrama, E., and Visser, P., Calibration and error assessment of GOCE data, in *Vistas for Geodesy in the New Millenium*, edited by J. Ádám and K.-P. Schwarz, vol. 125 of *International Association of Geodesy Symposia*, pp. 167–174, Springer, 2002.

Lemoine, F., Kenyon, S., Factor, J., Trimmer, R., Pavlis, N., Chinn, D., Cox, C., Klosko, S., Luthcke, S., Torrence, M., Wang, Y., Williamson, R., Pavlis, E., Rapp, R., and Olson, T., The development of the joint NASA GSFC and the National Imagery and Mapping Agency (NIMA) geopotential model EGM96, TP 1998-206861, NASA Goddard Space Flight Center, 1998.

Moritz, H., *Advanced physical geodesy*, Wichmann, 1980.

Müller, J., Jarecki, F., and Wolf, K., External calibration and validation of GOCE gradients, Accepted for publication in *Proceedings of the 3rd meeting of the IGGC*, 2002.

SID, GOCE End to End Performance Analysis, Final Report ESTEC Contract no 12735/98/NL/GD, SID, 2000.

Tscherning, C., A FORTRAN IV program for the determination of the anomalous potential using stepwise least squares collocation, Report No. 212, Department of Geodetic Science and Surveying, Ohio State University, 1974.

Tscherning, C., Covariance expressions for second and lower order derivatives of the anomalous potential, Report No. 225, Department of Geodetic Science and Surveying, Ohio State University, 1976.

Tscherning, C., Computation of covariances of derivatives of the anomalous gravity potential in a rotated reference frame, *Manuscripta Geodetica*, *8*, 115–123, 1993.